A Novel Tetrathiafulvalene- (TTF-) Fused Poly(aryleneethynylene) with an Acceptor Main Chain and Donor Side Chains: Intramolecular Charge Transfer (CT), Stacking Structure, and Photovoltaic Property

Yanhui Hou,[†] Yongsheng Chen,*[,†] Qian Liu,[‡] Min Yang,[§] Xiangjian Wan,[†] Shougen Yin,*[,‡] and Ao Yu[||]

Key Laboratory for Functional Polymer Materials and Centre for Nanoscale Science and Technology, Institute of Polymer Chemistry, College of Chemistry, Nankai University, Tianjin 300071, China, Institute of Material Physics, Tianjin University of Technology, Tianjin 300191, China, Institute of Polymer Science and Engineering, Hebei University of Technology, Tianjin 300130, China, Central Laboratory, College of Chemistry, Nankai University, Tianjin 300071, China

Received December 25, 2007; Revised Manuscript Received February 3, 2008

ABSTRACT: A novel tetrathiafulvalene- (TTF-) fused poly(aryleneethynylene) with an acceptor main chain and donor side chains has been prepared and characterized. The EPR and UV–vis spectra show that there exists intramolecular charge transfer (CT) between the electron-rich TTF side chains and the electron-deficient main chain. The band gaps deduced from UV–vis absorption spectroscopy and electrochemical studies are 1.78 and 1.84 eV, respectively. Powder X-ray diffraction analysis indicate that the polymer forms a self-assembled π-stacking structure and the polymer takes an interdigitation packing mode. Polymer solar cell has been fabricated with the blend of the TTF-fused polymer and C_{60} as the photosensitive layer. The power conversion efficiency is 0.25% under AM 1.5 simulated sun light (100 mW/cm^2). The intramolecular charge transfer was also confirmed by the chemical oxidation of the polymer with $Fe(bpy)_3(PF_6)_3$ (bpy = 2,2′-bipyridine).

Introduction

The design and synthesis of novel conjugated polymers attract great attention in the field of organic semiconductors due to their ease of preparation, low processing temperature, and nearly unlimited variability.[1] With the successful application of organic light-emitting diodes (OLEDs),[2] organic electronics is currently expanding its applications to organic photovoltaic devices (OPVDs)[3] and organic field effect transistors (OFETs).[4] For these device applications, the charge carrier mobility, band gap and electroactivity are the important parameters that should be considered in the design of conjugated polymers.[5] Combining TTF with linear π-conjugated polymers might be an exciting idea for developing the electroactive organic materials. From the viewpoint of tetrathiafulvalene (TTF) chemistry, TTF and its derivatives can exist in three stable states, which are TTF^0, $TTF^{\bullet+}$, and TTF^{2+}. Thus, grafting TTF redox centers on conjugated polymer may lead to a significant increase of their charge storage capacity.[6] Also, the TTF-fused polymers constitute highly polarizable species due to the large number of sulfur atoms in the structure. The extended conjugation could decrease the intramolecular Coulomb repulsive energy between the donor units and thus enhance intramolecular and interstack interactions.[7] Furthermore, the strong propensity of TTFs to self-assemble into regular π-stacks, when covalently attached to a π-conjugated backbone, may be an interesting approach for indirectly controlling the long-range order of the conjugated chain. The incorporation of TTF units into the conjugated polymers would increase the dimensionality of the charge transport, due to improved electron mobility along the polymer backbone via π-conjugation, as well as along the enhanced stacking direction via π-orbital overlap.[8]

There have been many reports on the preparation of conjugated polymers with TTF derivatives either in the main chains or in the side chain.[7,9] But for most of the polymers with TTF side chains, it is difficult to achieve the coplanarity of the main chain and the TTF units.[7a] In many cases, they can only have partial stacking for the TTF moieties, rather than continuous stacking of the whole molecules.[9a] Although the polymers with TTF-fused main chain can form the continuous stacks, they are generally labile to oxidation due to the strong electron-donating property of TTF units, resulting in poor performance when used in electronic or optoelectronic devices.[9d,10] Recently, Yamashita and co-workers found that introducing electron-deficient nitrogen heterocycles to the TTF skeleton could enhance the stability and charge mobility of the formed donor–acceptor (D–A) organic molecules.[10] At the same time, combining TTF donor and nitrogen acceptor heterocycle can effectively tailor the HOMO–LUMO gap. Moreover, it is of great benefit to obtain the ambipolar electroactivity by combining electron-donating and accepting abilities.[11] Herein, we report a novel TTF-fused D–A poly(*p*-aryleneethynylene), **PAE-TTF**, where the linear main chain acts as the electron-deficient acceptor and the π-conjugated TTF units act as the electron-rich donors in the side chains (Chart 1). The coplanarity of the main chain with the TTF units ensures that the polymer can easily form continuous stacks, which has been confirmed by the powder X-ray diffraction. EPR and UV–vis spectra of **PAE-TTF** show that there exists intramolecular charge transfer between the TTF side chains and the acceptor main chain. A photovoltaic device based on **PAE-TTF** has been fabricated and characterized.

Experimental Section

General Materials and Methods. Unless stated otherwise, all chemicals and reagents were purchased reagent-grade and used without further purification. Air and/or water-sensitive reactions were conducted under nitrogen using dry, freshly distilled solvents. 1,2-Diaminobenzene-4,5-bis(thiocyanate) (**1**),[12] 4,5-bis(dodecylthio)-1,3-dithiole-2-one (**3**),[13] 2,7-diiodophenanthrene-9,10-dione (**5**),[14] 4,7-bis(ethynyl)-2,1,3-benzothiadiazole (**7**),[15] and $Fe(bpy)_3(PF_6)_3$

* Corresponding author. Telephone: +86-22-23500693. Fax: +86-22-23499992. (Y.S.) E-mail: yschen99@nankai.edu.cn.
[†] Institute of Polymer Chemistry, College of Chemistry, Nankai University.
[‡] Tianjin University of Technology.
[§] Hebei University of Technology.
[||] Central Laboratory, College of Chemistry, Nankai University.

10.1021/ma702864c CCC: $40.75
Published on Web 04/02/2008

Chart 1. Molecular Structure of PAE-TTF[a]

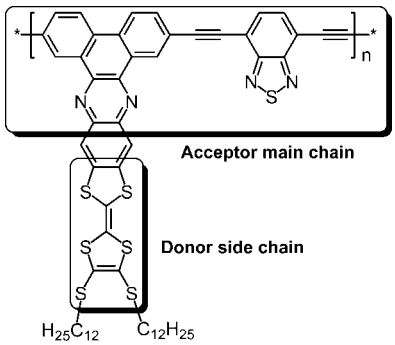

[a] Its linear main chain behaves as an electron-deficient acceptor, with the conjugated grafting electron-rich TTF units as the donors.

(bpy = 2,2′-bipyridine)[16] were prepared according to the literature procedures. ^{1}H NMR spectra were recorded on a Bruker AC-300 Spectrometer. Chemical shifts, δ, were reported in ppm relative to the internal standard TMS. Mass spectra (MS) were recorded using a Thermofinnigan LCQ Advantage mass spectrometer. Elemental analyses were performed on a Thermo Electron FLASH/EA 1112 instrument. Gel permeation chromatography (GPC) analysis was conducted on Polymer Laboratory PL-220. FT-IR spectra were recorded on Bruck Vector-22 spectrometer. Electron Paramagnetic Resonance (EPR) studies were performed with a Bruker EMX-6/1 spectrometer. Thermogravimetric analysis (TGA) measurement was performed on a TA instrument SDT-TG Q600 under an atmosphere of N_2 at a heat rate of 10 °C/min. Differential scanning calorimetric (DSC) measurement was recorded on a TA instrument DSC-2910, under an atmosphere of N_2 at a heat rate of 10 °C/min. Powder X-ray diffraction (XRD) was performed with a Rigaku X-ray diffractometer (D/max-2500).

Optical and Electrochemical Characterizations. UV–vis spectra were recorded on a JASCO-V570 spectrometer. Solid-state absorption spectrum was obtained on thin film coated on quartz prepared by spin-coating of the polymer saturated solution in *o*-dichlorobenzene. **PAE-TTF**$^{\bullet+}$ solution for EPR and UV–vis spectrum studies was obtained by chemical oxidation of **PAE-TTF** by $Fe(bpy)_3(PF_6)_3$. Cyclic voltammetry (CV) measurement was performed on a LK98B II Microcomputer-based Electrochemical Analyzer at room temperature with a three-electrode cell in a solution of Bu_4NPF_6 (0.1 M) in acetonitrile at a scanning rate of 100 mV/s. Polymer film was prepared via dipping the platinum working electrode into the polymer saturated solution and then drying under infrared lamp. A platinum wire was used as a counter electrode, and an $Ag/AgNO_3$ electrode was used as a reference electrode. After measurement, the reference electrode was calibrated with ferrocene (Fc) and the potential axis was corrected to Fc/Fc^+.

Photovoltaic Device Fabrication and Characterization. Conductive indium tin oxide (ITO) coated glass, $R_s = 15-30\ \Omega$ square^{-1}, was purchased from CSG Inc. The ITO-glass substrate was cleaned by ultrasonification sequentially in acetone, isopropyl alcohol, and deionized water. On top of the conductive side was coated a film of PEDOT:PSS (poly(ethylene dioxythiophene) doped with poly(styrenesulfonic acid) (Baytron P)). After being dried, this PEDOT:PSS film was covered with a layer of blend of **PAE-TTF**/C_{60} in a 2:1 w/w ratio by a spin-coating method from *o*-dichlorobenzene solution at 1000 rmp. The active layer was dried at 45 °C under vacuum for 1 h. The device was completed by evaporating a thin layer of LiF (ca. 1 nm thick) and a film of aluminum (ca. 100 nm thick) as the cathode in a two-step evaporation process under 3×10^{-4} Pa. The effective solar cell area was 8 mm^2 as defined by the geometrical overlap between the bottom ITO electrode and the top cathode. Device characterization was carried out under AM 1.5 G irradiation (100 mW/cm^2) on an Oriel Xenon solar simulator. The current–voltage ($I-V$) measurement of the photovoltaic device was conducted on a computer controlled Keithley 2400 Souce Measure Unit.

Synthesis of 5,6-diaminobenzene-1,3-dithiole-2-thione (2). The reported procedure[13] was modified as follows: 1,2-diaminobenzene-4,5-bis(thiocyanate) (2.44 g, 11 mmol) was added to a solution of $Na_2S{\bullet}9H_2O$ (8.71 g, 36 mmol) in water (135 mL), and the mixture was stirred for 1 h at 70 °C. After cooling to room temperature, CS_2 (1.2 mL, 20 mmol) was added. The mixture was stirred for 2 h at 45 °C. The precipitate was isolated by filtration, washed with water, and dried under vacuum to give 1.1 g of product (orange powder, yield: 48%), which is pure enough for the following synthesis and analysis. Mp: 211–213 °C. ^{1}H NMR (300 M, $(CD_3)_2SO$): $\delta = 6.81$ (s, 2H), 5.12 (s, 4H). ESI-MS (*m*/*z*): 215.3 ($M + H^+$). Anal. Calcd for $C_7H_6N_2S_3$: C, 39.23; H, 2.82; N, 13.07; S, 44.88. Found: C, 39.16; H, 2.78; N, 12.99; S, 45.07.

5,6-Diamino-2-(4,5-bis(dodecylthio)-1,3-dithiole-2-ylidene)-benzo[*d*]-1,3-dithiole (4). The reported procedure[17] was modified as follows: triethylphosphite (30 mL) was added slowly to a solution of compound 4,5-bis(dodecylthio)-1,3-dithiole-2-one (2.072 g, 4 mmol) and **2** (0.428 g, 2 mmol) in toluene (20 mL) under Ar. The mixture was stirred at 120 °C for 3 h. After the reaction, the excess solvent was removed under vacuum. The red residue was subjected to short basic Al_2O_3 column chromatography with a 1:1 mixture of CH_2Cl_2 and EtOAc as eluant, to give **4** as a yellow solid (0.438 g, 32%). Mp: 122–124 °C. ^{1}H NMR (300 M, $CDCl_3$): $\delta = 6.42$ (s, 2H), 4.53 (s, 4H), 2.82 (t, $J = 7.3$ Hz, 4H), 1.63 (m, 4H), 1.24 (m, 36H), 0.86 (t, $J = 7.3$ Hz, 6H). ESI-MS (*m*/*z*): 685.2 ($M + H^+$). Anal. Calcd for $C_{34}H_{56}N_2S_6$: C, 59.60; H, 8.24; N, 4.09; S, 28.08. Found: C, 59.51; H, 8.19; N, 4.14; S, 28.16.

4′,5′-Bis(dodecylthio)tetrathiafulvenyl-2,7-dionedibenzo[*a*,*c*]-phenazine (6). The mixture of compound **4** (0.343 g, 0.5 mmol) and **5** (0.23 g, 0.5 mmol) in 60 mL of ethanol was reflux for 3 h under N_2 and protected from light. After filtration, the precipitate was collected and purified by chromatography (basic Al_2O_3, CH_2Cl_2) to give **6** as a deep blue solid (0.377 g, 68%). Mp: 195–197 °C. ^{1}H NMR (300 M, *o*-$C_6D_4Cl_2$): $\delta = 9.27$ (s, 2H), 9.02 (d, $J = 8.1$ Hz, 2H), 8.28 (d, $J = 8.1$ Hz, 2H), 8.06 (s, 2H), 2.81 (t, $J = 7.3$ Hz, 4H), 1.61 (m, 4H), 1.24 (m, 36H), 0.86 (t, $J = 7.3$ Hz, 6H). APCI-MS (*m*/*z*): 1108.9 ($M + H^+$). FT-IR (KBr, cm^{-1}): 2922, 2851, 1587, 1431, 1346, 1204, 1091, 772. Anal. Calcd for $C_{48}H_{58}I_2N_2S_6$: C, 51.98; H, 5.27; N, 2.53; S, 17.35. Found: C, 52.05; H, 5.33; N, 2.58; S, 17.42.

Polymer PAE-TTF. Diisopropylamine (2 mL) was added to a mixture of compound **6** (0.111 g, 0.1 mmol), **7** (0.018 g, 0.1 mmol), $Pd(PPh_3)_4$ (0.012 g, 0.01 mmol), and CuI (0.002 g, 0.01 mmol) in 30 mL of THF under an argon atmosphere. The mixture was refluxed for 48 h. After being cooled to room temperature, the solid was collected by filtration and dissolved in as little 1,2,4-trichlorobenzene as possible. The solution was poured into DMF to give the desired **PAE-TTF** precipitate, which was separated by filtration and washed with methanol thoroughly (0.076 g, 74%). FT-IR (KBr, cm^{-1}): 2920, 2850, 2206, 1607, 1432, 1203, 1090, 777. GPC (eluent: 1,2,4-trichlorobenzene): $M_n = 6700$, DP = 6, PDI = 2.3. Anal. Calcd for $I(C_{58}H_{60}N_4S_7)_6$: C, 65.79; H, 5.73; N, 5.29; S, 21.20. Found: C, 66.53; H, 5.39; N, 5.96; S, 20.95.

Chemical Oxidization PAE-TTF for PAE-TTF$^{\bullet+}$**.** Excess $Fe(bpy)_3(PF_6)_3$ (0.67 g, 1 mmol) was added to a solution of **PAE-TTF** (0.01 g) in 10 mL of *o*-dichlorobenzene under N_2. The mixture was stirred in room temperature under dark for 1 h. After filtration, the **PAE-TTF**$^{\bullet+}$ solution was obtained, which was immediately used in the EPR and UV–vis spectra measurement.

Results and Discussion

Synthesis and Characterization. The synthetic pathway for monomer **6** is outlined in Scheme 1. The starting materials, **1**, **3**, and **5**, and another monomer, **7**, were synthesized according to the literature.[12–15] **2** was obtained by modifying the reported procedure.[13] By a phosphite-mediated cross-coupling reaction of **2** with **3**, the diamine TTF **4** could be obtained. Monomer **6** was easily obtained by direct condensation of **4** with **5**.

Scheme 1. Synthesis Schema of PAE-TTF[a]

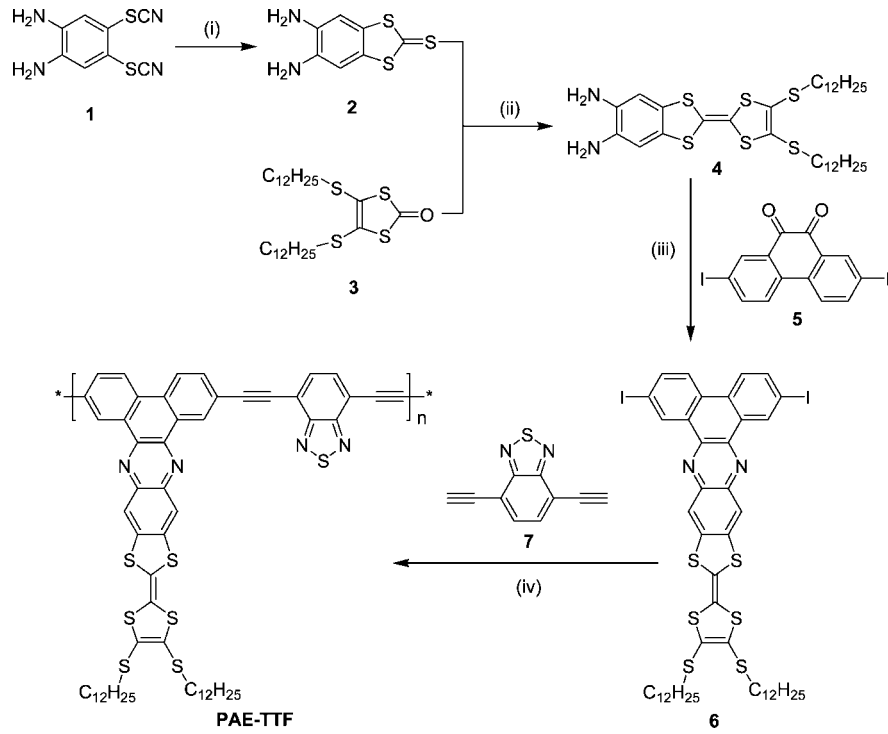

[a] Key: (i) NaS_2, H_2O, 70 °C, 1 h; CS_2, 45 °C, 2 h; (ii) $P(OEt)_3$, toluene, 120 °C, 3 h; (iii) ethanol, reflux, 3 h; (iv) $Pd(PPh_3)_4$, CuI, *i*-Pr_2NH, THF, reflux, 48 h.

Monomer **7** was very unstable and need to be prepared freshly before the following polymeric reaction for **PAE-TTF**. All compounds were purified and fully characterized.

The polymer, **PAE-TTF**, was synthesized through Sonogashira−Hagihara coupling reaction between the monomers **6** and **7** as described in Scheme 1. The obtained black-colored **PAE-TTF** is insoluble in tetrahydrofuran (THF) and $CHCl_3$. However, it can dissolve in *o*-dichlorobenzene and has a relative good solubility in 1,2,4-trichlorobenzene, too. The number averaged molecular weight, polydispersity and the degree of polymerization of the purified polymer **PAE-TTF** are M_n = 6700, PDI = 2.3, and DP = 6, respectively, using gel permeation chromatography (GPC) calibrated relative to polystyrene standards. We have tried to use different catalyst amount (3, 5, and 10%) for the polymerization. However, 10% catalyst gave the best result. In the process of polymerization, we found there was solid appearing in the reaction flask. The insolubility in THF results in the precipatation and may limit the molecular weight. Thus we tried to use 1,2,4-trichlorobenzene as the reaction solvent. Indeed the polymer had a relative high molecular weight (about 11000), but it only dissolved in 1,2,4-trichlorobenzene (the solar cells based on the polymer with a relatively high molecular weight had a much poorer performance, and other characters of the polymer have no obvious change, so for all the works in this paper, we used the polymer **PAE-TTF** synthesized with 10% catalyst in THF solvent as detailed in Scheme 1 and the Experimental Section).

FT-IR spectra of **PAE-TTF** and monomer **6** were shown in Figure 1. They are almost the same, and all exhibit absorption bands characteristic of the TTF units (e.g., 1430, 777 cm^{-1}). There appears a typical disubstituted acetylene ν(C≡C) peak at about 2200 cm^{-1} in the IR spectrum of **PAE-TTF**.[18] These are consistent with the proposed structure. However, the ^1H NMR spectrum of **PAE-TTF** only shows the hydrogen atoms of the two long alkyl chains. The hydrogen atoms on the aryl rings were not observed. Since it is expected that an efficient

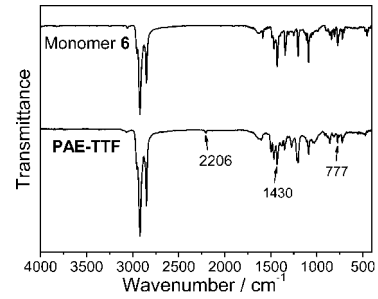

Figure 1. IR spectra of **PAE-TTF** and monomer **6** measured in the form of pressed KBr plates. They exhibit similar vibration peaks.

intramolecular charge transfer could happen between the electron-rich TTF and electron-deficient main chain in the polymer, we thus carried EPR studies for the fresh polymer under an Ar atmosphere. Indeed, the EPR spectrum of **PAE-TTF** solution in *o*-dichlorobenzene shows broad and weak signals (Figure 2a), which consist of the overlap of two resonance signals. One is a sharp signal with g = 2.005, the other is a broad signal with g = 2.001. Obviously, these paramagnetic species vanish the ^1H NMR peaks for the polymer mentioned above. Considering the oxidation instability of TTF moiety and the electron-deficient nature of the main chain, we suspect that there is possibly intramolecular electron-transfer between the side TTF units and main chain of **PAE-TTF** and radical ions may be generated (Figure 2b). To confirm this, we used $Fe(bpy)_3(PF_6)_3$ to oxidize **PAE-TTF.** The oxidation potential of $Fe(bpy)_3(PF_6)_3$ is 0.66 V,[19] which falls between the E_{ox1} and E_{ox2} of TTF units (see the electrochemical result below). Indeed, after addition of $Fe(bpy)_3(PF_6)_3$ to the solution of **PAE-TTF**, a sharp EPR signal showed up with g = 2.005 (Figure 2c). This EPR spectrum is in line with the characteristic EPR signal of the cation radical $TTF^{\bullet 1+}$ units.[5c,9a] Thus we believe that the oxidation of **PAE-TTF** by $Fe(bpy)_3(PF_6)_3$ generated

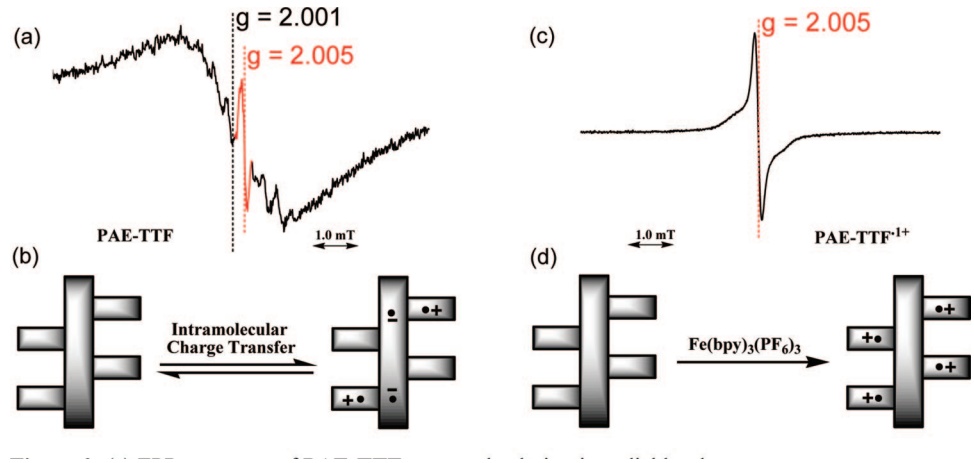

Figure 2. (a) EPR spectrum of **PAE-TTF** saturated solution in *o*-dichlorobenzene at room temperature. (b) Cartoon representation of intramolecular charge transfer beteen electron-rich TTF side chains and electron-deficient main chain of **PAE-TTF**. (c) EPR spectrum of **PAE-TTF**$^{\bullet 1+}$ solution in o-dichlorobenzene at room temperature prepared by $Fe(bpy)_3(PF_6)_3$ oxidation. (d) Cartoon representation of the oxidation of **PAE-TTF** by $Fe(bpy)_3(PF_6)_3$ to form **PAE-TTF**$^{\bullet+}$. Parts b and d correspond to parts a and c, respectively.

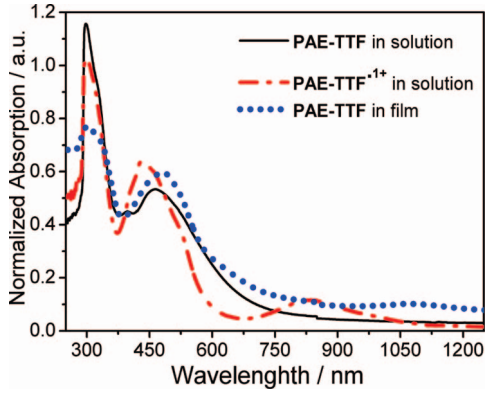

Figure 3. UV–vis absorption spectra of **PAE-TTF, PAE-TTF**$^{\bullet+}$ solution in *o*-dichlorobenzene (3×10^{-5} M of the repeat unit) and **PAE-TTF** film on quartz plates (film from *o*-dichlorobenzene saturated solution). **PAE-TTF**$^{\bullet+}$ solution was obtained by chemical oxidation of **PAE-TTF** by $Fe(bpy)_3(PF_6)_3$.

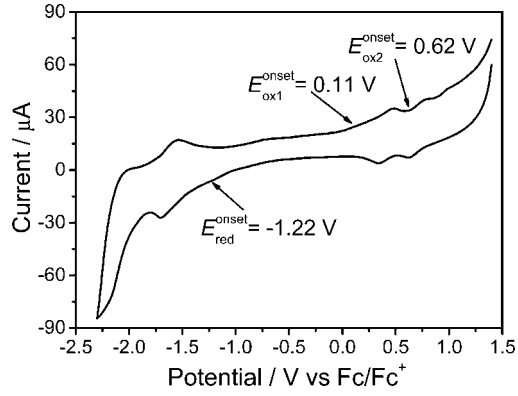

Figure 4. Cyclic voltammograms of **PAE-TTF** film on platinum plates in acetonitrile solution of 0.1 M Bu_4NPF_6 with a potential scanning rate of 0.1V/s at room temperature and potential vs Fc/Fc^+. The **PAE-TTF** film was prepared via dipping the platinum working electrode into the polymer-saturated solution in *o*-dichlorobenzene and then drying under an infrared lamp.

the radical cation **PAE-TTF**$^{\bullet+}$, which gave a typical EPR spectrum of TTF$^{\bullet+}$. This also indicates that the first oxidation wave of **PAE-TTF** in its CV (see below) should happen on the TTF side chain moiety of the polymer **PAE-TTF.** So we believe that the sharp signal with $g = 2.005$ in the EPR spectrum of **PAE-TTF** is from the TTF$^{\bullet+}$ units. The broad signal probably

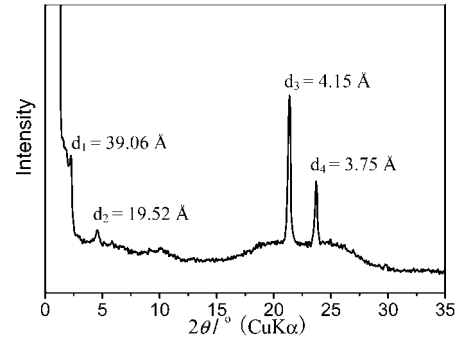

Figure 5. X-ray diffraction patterns of **PAE-TTF** powder. Peaks are labeled with *d*-spacing in angstroms. The sharp diffraction peaks indicate that the polymer formed an ordered structure in the solid state.

comes from the spin resonance of the accepted single electrons in the main chain.

The thermogravimetric analysis (TGA) in the inert nitrogen atmosphere reveals that the onset temperature of the weight loss of **PAE-TTF** is about 230 °C (not shown). It is apparent that the polymer is stable enough to be fabricated into a device and measured at ambient conditions. Differential scanning calorimetry (DSC) measurement of the polymer was also conducted. There was no obvious thermal transition observed below 230 °C, indicating that the polymer is so rigid that the T_g is higher than the decomposition temperature.

UV–Vis Properties. The UV–vis absorption spectra of **PAE-TTF** solution in o-dichlorobenzene and film on quartz plate are shown in Figure 3. The spectra all have one absorption peak about at 300 nm in the ultraviolet (UV) region, which is attributed to the absorption of the long alkyl chains.[20] There is a broad absorption in the visible region (~400 – 800 nm) for the **PAE-TTF** solution and film. In this region, the absorption peak of the **PAE-TTF** solution is located at 460 nm. The broad shape in the visible region is also an indication of the intramolecular charge transfer character between the side chain donor TTF units and the central acceptor main chain.[11] In comparison with the absorption spectrum of the polymer solution, the absorption of the film in the visible region becomes bathochromically shifted by about 20 nm, indicating that in the solid film the interchain interactions make main chains from the π-stacking (see also the XRD below). This phenomenon has been observed in other similar conjugated polymers.[20] The optical band gap (E_g^{opt}) of **PAE-TTF** was estimated to be 1.78

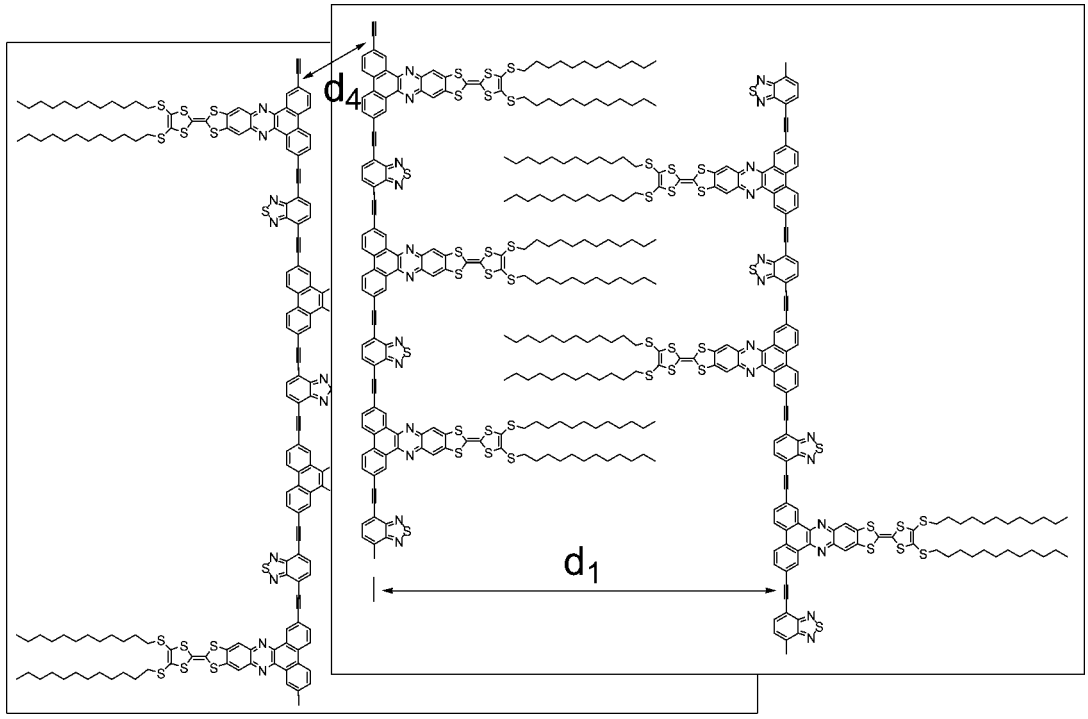

Figure 6. Schematic representation of a proposed packing structure of **PAE-TTF** in solid state. The polymer with long side chains assumes an interdigitation packing mode; the segregation of the polymer main chains accounts for the interchain d_1 spacing. d_4 represents the π-stacking distance between the coplanar backbones.

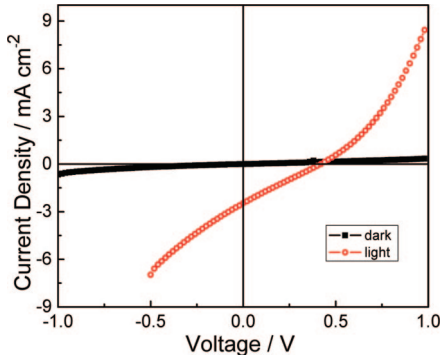

Figure 7. Current–voltage characteristics of the ITO/PEDOT:PSS/**PAE-TTF**:C_{60} (2:1w/w)/LiF/Al solar cell measured in the dark and under AM 1.5 illumination (100 mW/cm^2). Open-circuit voltage (V_{oc}) and short-circuit current (I_{sc}) are 0.42 V and 2.47 mA/cm^2, respectively.

eV from its absorption edge. The UV–vis absorption spectrum of **PAE-TTF**$^{\bullet+}$ solution in *o*-dichlorobenzene is also shown in Figure 3. Obviously, there appears a new broad absorption between 700 and 1000 nm, which is the characteristic of the cation radical TTF$^{\bullet+}$.[17,21] Also, the absorption between 400–800 nm of **PAE-TTF** solution become narrowed to 400–600 nm for **PAE-TTF**$^{\bullet+}$ and hypsochromically shifted.

Electrochemical Property. The electrochemical property of **PAE-TTF** was investigated by cyclic voltammetry (CV). Figure 4 shows the cyclic voltammogram of its thin-film on a Pt electrode in a 0.1 M Bu_4NPF_6 acetonitrile solution. The polymer shows two reversible single electron oxidation waves about at $E_{1/2}^{ox1} = 0.47$ and $E_{1/2}^{ox2} = 0.78$ V, corresponding to the typical redox peaks of the TTF units.[17,21] The first oxidation should be attributed to the bis(thioether)-substituted half-unit, while the second arises from the phenazinedithiol moiety.[22] This assignment is justified by the electron withdrawing effect of the main chain. Moreover, the polymer has a quasi-reversible reduction process about at –1.7 V, which can be assigned to reduction of the acceptor main chain.[17,22] The redox property of **PAE-TTF** is similar to that of other similar TTF-fused D–A ensembles.[17,21]

For simple conjugated polymers, the difference between the onset of the first oxidation peak and the reduction peak corresponds to be the electrochemical band gap. Using the first oxidation process for **PAE-TTF**, this band gap value might be approximately 1.33 eV, obviously less than that determined by UV–vis absorption spectroscopy. However, Skabara et al. thought since this redox event came from the first oxidation (attributed to the bis(thioether)-substituted dithiol unit) and it is believed that this electrochemical process is independent of the conjugated main chain.[5c,22] Thus the onset of the second oxidation peak should be used in the determination of the band gap value.[5c,22] So the obtained value of **PAE-TTF**, using the onset of the second oxidation peak, is 1.84 eV, which is close to that determined by the UV–vis absorption spectroscopy above.

X-ray Diffraction. To investigate the crystallinity of the polymer in the solid state, X-ray diffraction (XRD) pattern was collected on a powder sample of the polymer (Figure 5). The diffraction peak at 2θ of 2.26°, corresponding to spacing $d_1 =$ 39.06 Å, is assigned to a distance between the conjugated main chains separated by the long side chains as reported for other similar π-conjugated polymers with long side chains.[23] However, the length of the rigid portion of the side chain is about 15 Å. Adding the two long alkyl chains, the total length of the side chain will reach 29 Å. If the polymer took the end-to-end packing mode, d_1 should be 58 Å, which is far larger than the observed 39.06 Å. So the polymer is considered to assume an interdigitation packing mode rather than an end-to-end packing mode (Figure 6). The diffraction peak d_2 is the second-order peak ($d_2 = d_1/2$) of the diffraction at d_1.[23]

The effective cross section of the alkyl chains is about $S =$ 20 Å and their hexagonal-like aggregation gives about $d = 4.2$ Å.[24] This value is in agreement with what we observed for the peak at d_3 (4.15 Å) from the polymer. The value of d_4 observed is close to the π-stacking distances of reported TTF-fused D–A organic compounds, which were observed from their single

crystal structures.[10,17] So d_4 is considered to be the layer-to-layer π-stacking distance between the coplanar backbones. This value is somewhat larger than the sheet-to-sheet distance of graphite (3.35 Å).[24] The diffraction peaks of d_1-d_4 was often observed in the X-ray diffraction patterns of poly(aryleneethynylene)s.[25] On the basis of these results, we can suspect that, in the solid state, **PAE-TTF** forms a good face-to-face stacking consisting of both the π-extended coplanar backbones and the crystallinity of the long alkyl chains.

Photovoltaic Property. The intramolecular charge transfer between the TTF side chains and the acceptor main chain and good π-stacking of **PAE-TTF** indicate that it could possess photovoltaic properties. So we fabricated the polymer solar cell (PSCs) with a structure of ITO/PEDOT:PSS/**PAE-TTF**:C_{60} (2:1 w/w)/LiF/Al. Figure 7 shows $I-V$ curves of the device based on **PAE-TTF** in dark and under the white light illumination (AM 1.5, 100 mW/cm^2). Preliminary results showed that the corresponding open-circuit voltage (V_{oc}), short-circuit current (I_{sc}), fill factor (FF), and power conversion efficiency (PCE) of the device were 0.42 V, 2.47 mA/cm^2, 24.2%, and 0.25%, respectively. Although the power conversion efficiency is relative low, to our best knowledge, it excels that of other reported TTF-fused ensembles.[5c,26] The intramolecular charge transfer between the TTF side chains and the acceptor main chain could help the exciton charge separation, which may be the reason for the increasing of the power conversion efficiency. We are currently optimizing the polymer and device for better photovoltaic performance.

Conclusion

In summary, we have prepared a novel tetrathiafulvalene-(TTF-) fused poly(aryleneethynylene) with an acceptor main chain and donor side chains. There exists intramolecular charge transfer (CT) between the electron-rich TTF side chains and the electron-deficient main chain. The electroactivity of the TTF units is closely associated with the HOMO–LUMO levels of the conjugated polymer. The coplanarity of the acceptor main chain and the donor TTF side chains ensures that the polymer forms effective π-π stacking in the solid state. Initial studies showed the photovoltaic property of the polymer **PAE-TTF** had significant improvement compared with that of other TTF-fused polymer analogues. The lack of effective absorption in red to near-infrared region of the sun spectrum may result in the still low power conversion efficiency, but the intramolecular charge transfer and good π-stacking indicate that this kind of TTF-fused polymers may become a promising active material for photovoltaic and other organic electronic devices.

Acknowledgment. We gratefully acknowledge the financial support from the NSFC (No. 20644004, No. 20774047), MoST (No. 2006CB932702), and NSF of Tianjin City (Nos. 07JCYBJC03000 and 06TXTJJC14603).

References and Notes

(1) (a) Roncali, J.; Leriche, P.; Cravino, A. *Adv. Mater.* **2007**, *19*, 2045–2060. (b) Kertesz, M.; Choi, C. H.; Yang, S. *Chem. Rev.* **2005**, *105*, 3448–3481. (c) Li, Z.; Qin, A.; Lam, J. W. Y.; Dong, Y.; Dong, Y.; Ye, C.; Williams, I. D.; Tang, B. Z. *Macromolecules* **2006**, *39*, 1436–1442. (d) Brédas, J. L.; Beljonne, D.; Coropceanu, V.; Cornil, J. *Chem. Rev.* **2004**, *104*, 4971–5004.

(2) (a) D'Andrade, B. *Nature Photonics* **2007**, *1*, 33–34. (b) Perepichka, I. F.; Perepichka, D. F.; Meng, H.; Wudl, F. *Adv. Mater.* **2005**, *17*, 2281–2305.

(3) (a) Günes, S.; Neugebauer, H.; Sariciftci, N. S. *Chem. Rev.* **2007**, *107*, 1324–1338. (b) Coakley, K. M.; McGehee, M. D. *Chem. Mater.* **2004**, *16*, 4533–4542.

(4) (a) Murphy, A. R.; Fréchet, J. M. J. *Chem. Rev.* **2007**, *107*, 1066–1096. (b) Chua, L. L.; Zaumseil, J.; Chang, J. F.; Ou, E. C. W.; Ho, P. K. H.; Sirringhaus, H.; Friend, R. H. *Nature* **2005**, *434*, 194–199.

(5) (a) Zhu, Z.; Waller, D.; Gaudiana, R.; Morana, M.; Mühlbacher, D.; Scharber, M.; Brabec, C. *Macromolecules* **2007**, *40*, 1981–1986. (b) Scharber, M. C.; Mühlbacher, D.; Koppe, M.; Denk, P.; Waldauf, C.; Heeger, A. J.; Brabec, C. L. *Adv. Mater.* **2006**, *18*, 789–794. (c) Berridge, R.; Skabara, P. J.; Pozo-Gonzalo, C.; Kanibolotsky, A.; Lohr, J.; McDouall, J. J. W.; McInnes, E. J. L.; Wolowska, J.; Winder, C.; Sariciftci, N. S.; Harrington, R. W.; Clegg, W. J. *Phys. Chem. B* **2006**, *110*, 3140–3152. (d) Reference deleted in proof.

(6) (a) Wudl, F.; Wobschall, D.; Hufnagel, E. J. *Am. Chem. Soc.* **1972**, *94*, 670–672. (b) Wang, E.; Li, H.; Hu, W.; Zhu, D. J. *Polym. Sci., Part A: Polym. Chem.* **2006**, *44*, 2707–2713.

(7) (a) Inagi, S.; Naka, K.; Chujo, Y. J. *Mater. Chem.* **2007**, *17*, 4122–4135. (b) Wudl, F. *Acc. Chem. Res.* **1984**, *17*, 227–232.

(8) (a) Segura, J. L.; Martín, N. *Angew. Chem., Int. Ed.* **2001**, *40*, 1372–1409. (b) Huchet, L.; Akoudad, S.; Roncali, J. *Adv. Mater.* **1998**, *10*, 541–545. (c) Adam, M.; Müllen, K. *Adv. Mater.* **1994**, *6*, 439–459.

(9) (a) Gomar-Nadal, E.; Mugica, L.; Vidal-Gancedo, J.; Casado, J.; Navarrete, J. T. L.; Veciana, J.; Rovira, C.; Amabilino, D. B. *Macromolecules* **2007**, *40*, 7521–7531. (b) Lyskawa, J.; Derf, F. L.; Levillian, E.; Mazari, M.; Sallé, M.; Dubois, L.; Viel, P.; Bureau, C.; Palacin, S. *J. Am. Chem. Soc.* **2004**, *126*, 12194–12195. (c) Shimada, S.; Masaki, A.; Hayamizu, K.; Matsuda, H.; Okada, S.; Nakanishi, H. *Chem. Commun.* **1997**, 1421–1422. (d) Uemura, T.; Naka, K.; Chujo, Y. *Adv. Polym. Sci.* **2004**, *167*, 81–106.

(10) (a) Naraso; Nishida, J.; Kumaki, D.; Tokito, S.; Yamashita, Y. *J. Am. Chem. Soc.* **2006**, *128*, 9598–9599. (b) Naraso; Nishida, J.; Ando, S.; Yamaguchi, J.; Itaka, K.; Koinuma, H.; Tada, H.; Tokito, S.; Yamashita, Y. *J. Am. Chem. Soc.* **2005**, *127*, 10142–10143.

(11) Casado, J.; Ortiz, R. P.; Delgado, M. C. R.; Hernández, V.; Navarrete, J. T. L. J. *Phys. Chem. B* **2005**, *109*, 16616–16627.

(12) Brusso, J. L.; Clements, O. P.; Haddon, R. C.; Itkis, M. E.; Leitch, A. A.; Oakely, R. T.; Reed, R. W.; Richardson, J. F. J. *Am. Chem. Soc.* **2004**, *126*, 8256–8265.

(13) Frei, M.; Diederich, F.; Tremont, R.; Rodriguez, T.; Echegoyen, L. *Helv. Chim. Acta* **2006**, *89*, 2040–2057.

(14) Luliński, P.; Skulski, L. *Bull. Chem. Soc. Jpn.* **1999**, *72*, 115–120.

(15) Neto, B. A. D.; Lopes, A. S. A.; Ebeling, G.; Gonçalves, R. S.; Costa, V. E. U.; Quina, F. H.; Dupont, J. *Tetrahedron* **2005**, *61*, 10975–10982.

(16) Lemmen, T. H.; Lundquist, E. G.; Rhodes, L. F.; Sutherland, B. R.; Westerberg, D. E.; Caulton, K. G. *Inorg. Chem.* **1986**, *25*, 3915–3917.

(17) Jia, C.; Liu, S. X.; Tanner, C.; Leiggener, C.; Neels, A.; Sanguinet, L.; Levillain, E.; Leutwyler, S.; Hauser, A.; Decurtins, S. *Chem. Eur. J.* **2007**, *13*, 3804–3812.

(18) (a) Fang, Q.; Ren, S.; Xu, B.; Du, J.; Cao, A. J. *Polym. Sci., Part A: Polym. Chem.* **2006**, *44*, 3797–3806. (b) Shimizu, T.; Yamamoto, T. *Chem. Commun.* **1999**, 515–516.

(19) Connelly, N. G.; Geiger, W. E. *Chem. Rev.* **1996**, *96*, 877–910.

(20) (a) Zhou, E.; He, C.; Tan, Z.; Yang, C.; Li, Y. J. *Polym. Sci., Part A: Polym. Chem.* **2006**, *44*, 4916–4922. (b) Ashraf, R. S.; Shahid, M.; Klemm, E.; Al-Ibrahim, M.; Sensfuss, S. *Marcromol. Rapid Commun.* **2006**, *27*, 1454–1459.

(21) Jia, C.; Liu, S. X.; Tanner, C.; Leiggener, C.; Sanguinet, L.; Levillain, E.; Leutwyler, S.; Hauser, A.; Decurtins, S. *Chem. Commun.* **2006**, 1878–1880.

(22) Skabara, P. J.; Berridge, R.; McInnes, E. J. L.; West, D. P.; Coles, S. J.; Hursthouse, M. B.; Müllen, K. *J. Mater. Chem.* **2004**, *14*, 1964–1969.

(23) Yamamoto, T.; Lee, B. L. *Macromolecules* **2002**, *35*, 2993–2999.

(24) Yamamoto, T.; Arai, M.; Kokubo, H.; Sasaki, S. *Macromolecules* **2003**, *36*, 7986–7993.

(25) (a) Yasuda, T.; Imase, T.; Nakamura, Y.; Yamamoto, T. *Macromolecules* **2005**, *38*, 4687–4697. (b) Bangcuyo, C. G.; Evans, U.; Myrick, M. L.; Bunz, U. H. F. *Macromolecules* **2001**, *34*, 7592–7594. (c) Morikita, T.; Yamaguchi, I.; Yamamoto, T. *Adv. Mater.* **2001**, *13*, 1862–1864. (d) Yamamoto, T.; Kokubo, H; Morikita, T. *J. Polym. Sci., Part B: Polym. Phys.* **2001**, *39*, 1713–1718.

(26) Martín, N.; Sánchez, L.; Herranz, M.Á.; Illescas, B.; Guldi, D. M. *Acc. Chem. Res.* **2007**, *40*, 1015–1024.

MA702864C